JACS
JOURNAL OF THE AMERICAN CHEMICAL SOCIETY

COMMUNICATION

pubs.acs.org/JACS

Synthesis of Shape-Controlled Monodisperse Wurtzite $CuIn_xGa_{1-x}S_2$ Semiconductor Nanocrystals with Tunable Band Gap

Yu-Hsiang A. Wang,[*,†] Xiaoyan Zhang,[†,‡] Ningzhong Bao,[*,†,§] Baoping Lin,[‡] and Arunava Gupta[*,†]

[†]Center for Materials for Information Technology, University of Alabama, Tuscaloosa, Alabama 35487, United States

[‡]School of Chemistry and Chemical Engineering, Southeast University, Nanjing, P. R. China

[§]State Key Laboratory of Materials-Oriented Chemical Engineering, Nanjing University of Technology, Nanjing, P. R. China

Supporting Information

ABSTRACT: Monodisperse wurtzite $CuIn_xGa_{1-x}S_2$ nanocrystals have been synthesized over the entire composition range using a facile solution-based method. Depending on the chemical composition and synthesis conditions, the morphology of the nanocrystals can be controlled in the form of bullet-like, rod-like, and tadpole-like shapes. The band gap of the nanocrystals increases linearly with increasing Ga concentration, with band gap values for the end members being close to those observed in the bulk. Colloidal suspensions of the nanocrystals are attractive for use as inks for low-cost fabrication of thin film solar cells by spin or spray coating.

With ever increasing demand for clean energy, the fabrication of low cost and high efficiency photovoltaic devices has attracted considerable attention in recent years. Among different types of photovoltaic devices, inorganic photovoltaic cells have exhibited the highest solar energy conversion efficiency, but at the expense of high fabrication cost. A possible approach for reducing cost is to use colloidal nanocrystals synthesized using simple solution-based methods. Recently, there have been a number of reports on the fabrication of thin film solar cells by spin coating[1] and screen printing[2] of colloidal semiconducting nanocrystals, with an efficiency as high as 7.2% being reported using copper−zinc−tin−chalcogenide nanocrystals.[3] Besides chemical composition and crystal phase, the band gap of semiconductor nanocrystals can be tuned by varying the size because of the quantum confinement effect.[4] Moreover, the nanocrystal shape can influence their optical properties. For example, one-dimensional nanorods and nanowires have been observed to exhibit optical properties that are different from those of quantum dots.[5] Therefore, systematic tuning of the composition, crystal phase, size, and shape of semiconducting nanocrystals represents an attractive approach for developing next-generation, low-cost, and high-performance solar cells.

Among different classes of semiconducting materials, $A^+B^{3+}X^{2-}{}_2$ semiconductors of the I−III−VI_2 family, such as $CuIn_xGa_{1-x}S(Se)_2$, are of considerable interest for use as light-emitting diodes, photovoltaic cells, and nonlinear optical devices.[6] The most common crystal structure of $A^+B^{3+}X^{2-}{}_2$ semiconductors is chalcopyrite, in which the A and B ions are ordered in the cation sublattice sites. Random distribution of the cations leads to the zinc blende structure.[7] The orthorhombic phase is another ordered phase of $A^+B^{3+}X^{2-}{}_2$ that has been observed for $AgInS_2$ and $AgInSe_2$.[8] Similar to the chalcopyrite structure, when the A and B ions are disordered in the cation sites, the orthorhombic phase converts to a wurtzite structure. The random distribution of A and B ions in the wurtzite phase offers flexibility for stoichiometry control, which is advantageous for fabrication of photovoltaics[9a] since it provides the ability to tune the Fermi energy over a wide range.[9b] For example, as one of the end members, $CuInS_2$ (CIS) has proven to be effective for fabricating high efficiency thin film solar cells because of its unique properties such as high absorption efficiency,[10] a direct band gap,[11] facile electron/hole carrier conversion,[12] and being eco-friendly.

Unlike binary chalcogenides,[13] the synthesis of ternary CIS and, in particular, quaternary $CuIn_xGa_{1-x}S_2$ (CIGS) nanocrystals is challenging because of the difficulty in controlling the stoichiometry and phase structure. Recently, $CuInS_2$ nanocrystals with crystal phases in the form of chalcopyrite,[14] zinc-blende,[15] and wurtzite[9,16] structures have been successfully synthesized using solvothermal and other conventional solution synthesis methods. Monodisperse CIS nanocrystals with different morphologies have been obtained with a variable ratio of copper and indium.[16a] Chalcopyite phase $CuGaS_2$ (CGS) nanocrystals have also been synthesized by hydrothermal and solvothermal methods.[17] However, the product is mostly in the form of large crystallites with a broad size distribution. Similarly, for quaternary CIGS, only the synthesis of chalcopyrite phase nanocrystals has been reported.[18] To the best of our knowledge, wurtzite-structured $CuIn_xGa_{1-x}S_2$ nanocrystals have not been synthesized for values of $x < 1$. Herein we report on the facile synthesis of wurtzite-structured CIGS nanocrystals with controlled morphology and narrow size distribution over the entire composition range ($0 \le x \le 1$). The band gap can be systematically tuned by varying the In/Ga ratio, and the nanocrystals readily form colloidal suspensions that are attractive for fabrication of solar cells.

All reactions were performed in a fume hood, under inert conditions. In a typical reaction for the synthesis of CIGS nanocrystals with the wurtzite structure, 1 mmol of copper(II) acetylacetonate (acac), 1 mmol of indium(III)/gallium(III) acetylacetonate (acac), and 3.5 mmol of trioctylphosphine oxide (TOPO) (90%) were mixed with 10 mL of oleylamine in a four-neck round-bottom flask and stirred at room temperature for

Received: April 28, 2011
Published: June 24, 2011

30 min with nitrogen purging. The solution was then heated to 150 °C, and a mixture of 0.25 mL of 1-dodecanethiol (1-DDT) and 1.75 mL of *tert*-dodecanethiol (t-DDT) was rapidly injected into the solution under a nitrogen atmosphere with continuous stirring. The solution turned essentially clear with a light yellow color. The solution mixture was then heated up to 280−290 °C in 30 min and maintained at this temperature for 30 min. The mixture was subsequently cooled down to room temperature, and a mixture of hexane and ethanol was used to precipitate the product and collect it via centrifugation. The color of the centrifuged product varied from black for $CuInS_2$, dark red for $CuIn_{0.5}Ga_{0.5}S_2$, to dark yellow for $CuGaS_2$. A similar procedure was used for the synthesis of tadpole-shaped nanocrystals. The only difference being that the metal acetylacetonate precursors were initially dissolved in 10 mL of 1-octadecene (ODE) instead of oleylamine (OLA).

We have determined that the optimal temperature for injecting the 1-DDT and t-DDT solution into the copper/indium/gallium precursor solution is around 150 °C. Kruszynska et al.[16d] synthesized CIS nanocrystals by injecting the sulfur source at temperatures above 200 °C and observed formation of Cu_2S as an impurity phase in the product mixture. Han et al.[19] reported the synthesis of Cu_2S particles using $Cu(acac)_2$ and dodecanethiol as precursors. With increasing temperature, the precursor solution turned clear at 148−152 °C and then quickly precipitated Cu_2S particles at 200 °C. These results suggest that in order to avoid formation of the Cu_2S phases the optimal temperature for the synthesis of CIS nanocrystals should be below 200 °C. Therefore, our strategy for avoiding the formation of Cu_2S was to first form the intermediate $CuInGa(SR)_x$ complexes before the reaction system goes through the formation temperature of Cu_2S at 200 °C. $In(acac)_3$ and $Ga(acac)_3$ were specifically chosen as reactants because of their low decomposition temperature.[20] Accordingly, we added a step involving aging of the reactants at 150 °C for 30 min. This enables the formation of intermediate complexes as confirmed by a color change to light yellow. These intermediates likely result in the formation of stoichiometric CIGS clusters that can then grow during the subsequent step of fast heat-up and short aging at 280−290 °C. This is similar to the reported synthesis of ternary chalcogenide nanocrystals using single source precursors.[8c,21] Note that the reaction time for synthesis of CIS nanocrystals using our procedure is much shorter than that reported (17−24 h) for converting the biphasic Cu_2S-$CuInS_2$ to monophasic $CuInS_2$ nanocrystals.[16d] Thus, quaternary $CuIn_xGa_{1-x}S_2$ (CIGS) nanocrystals, instead of Cu_2S or mixed phases, can be efficiently synthesized by first mixing and forming a clear solution mixture of the intermediates at 150 °C and then heating up the mixture to a temperature of 280−290 °C for product formation.

The morphology of the synthesized products has been investigated using TEM. As seen in Figure 1a, the CIS nanocrystals synthesized in OLA have a bullet-like shape with a uniform size of about 16 nm in width and 35 nm in length. For nanocrystals with a composition of $CuIn_{0.75}Ga_{0.25}S_2$, the shape changes to rod-like and their average length is smaller. As a general trend, a decrease in the average size of the nanocrystals is observed with increasing concentration of Ga (Figure S1). By replacing OLA with ODE as the solvent, the morphology of CIGS changes from nanobullet to nanorod (Figure 1b), nanosphere, and nanotadpole (Figure 1c) shape. Both CGS and $CuIn_{0.25}Ga_{0.75}S_2$ nanocrystals exhibit a tadpole-like shape, with the $CuIn_{0.25}Ga_{0.75}S_2$ nanotadpoles being relatively smaller in size (see Figure S2). The morphology variations

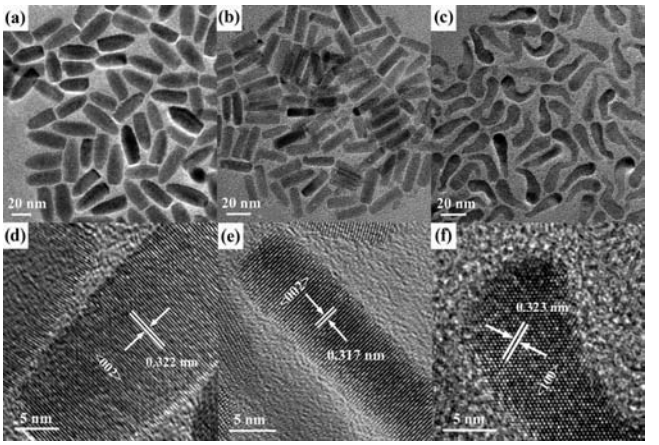

Figure 1. TEM images of (a) bullet-like $CuInS_2$ nanocrystals synthesized in OLA, (b) rod-like $CuIn_{0.75}Ga_{0.25}S_2$ nanocrystals synthesized in ODE, and (c) tadpole-like $CuGaS_2$ nanocrystals synthesized in ODE; HRTEM images of individual (d) bullet-like, (e) rod-like, and (f) tadpole-like nanocrystals.

with different Ga/In ratios is likely caused by differences in the binding strength of the respective cations with TOPO.[22] The weaker binding of Ga^{3+} can result in a broader size distribution with increasing Ga concentration in CIGS, as has been observed. Similarly, the observed changes in the shape and size of the nanocrystals using OLA and ODE as solvents can be attributed to differences in their coordination ability with the cations, with OLA known to be a much stronger coordinating ligand than ODE.[23]

HRTEM images of individual nanocrystals for the different shapes show clear lattice fringes with spacings of $d = 0.322 \pm 0.004$ nm (Figure 1d) and $d = 0.317 \pm 0.005$ nm (Figure 1e), corresponding to the (002) lattice plane of the wurtzite structure. One-dimensional wurtzite ZnO[24] and CdSe[25] nanorods also display preferential growth along the [001] direction. Lattice fringes shown in Figure 1f have an average spacing of $d = 0.323 \pm 0.005$ nm, corresponding to (100) lattice planes of the wurtzite structure. The d spacing measured in the tail section of a typical tadpole-like nanocrystal is the same as that in the head part, indicating the same wurtzite structure (Figure S3). Similar nanotadpole-shape growth has been reported for CdSe,[25] $AgInSe_2$,[26] and gold[27] nanocrystals. We have not observed any significant lattice distortion in the CGS nanotadpoles by HRTEM (Figure S3). While the formation mechanism of the tail segment of the nanocrystals is not totally clear, it can partly be attributed to the random growth along the [100] and [010] directions in the hexagonal structure.

Figure 2 shows the XRD patterns of CIGS nanocrystals of different compositions. Major diffraction peaks for CIS nanocrystals (Figure 2a) are observed at 2θ values of 26.24°, 27.67°, 29.74°, 38.56°, 46.40°, and 50.34°. The peak positions and relative peak intensities match well with the powder diffraction data reported for wurtzite $CuInS_2$.[16] Because of the smaller size of a gallium ion as compared to indium, a systematic shift of the peaks to higher angles is noted with increasing gallium substitution (Figure 2a to 2e). The chalcopyrite phase is thermodynamically more stable than the wurtzite phase in the bulk as indicated by both experimental results[28] and theoretical calculations.[29] For the synthesis of wurtzite CIS nanocrystals, both dodecanethiol and oleylamine are strong coordinating ligands

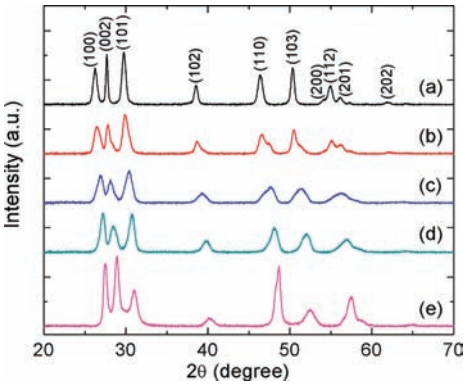

Figure 2. XRD patterns of the wurtzite phase of (a) $CuInS_2$, (b) $CuIn_{0.75}Ga_{0.25}S_2$, (c) $CuIn_{0.5}Ga_{0.5}S_2$, (d) $CuIn_{0.25}Ga_{0.75}S_2$, and (e) $CuGaS_2$ nanocrystals synthesized in OLA.

that can bind onto the surface of nanocrystals and thus decrease the surface energy for stabilizing the wurtzite phase. Such 'ligand effect' has been observed in experimental studies of the synthesis of wurtzite copper-based chalcogenide nanocrystals.[9a,16a,30] Besides ligand effect, other factors such as the nature of the sulfur source and its decomposition rate, the presence of coordinating solvents, reaction temperature, and concentration of metal reactants in solution are also known to strongly influence the formation of metastable wurtzite CIS nanocrystals.[9,16] Thus, a combination of kinetic factors are responsible for the preferential growth and stability of the wurtzite phase.

Besides the composition, the relative intensities of the primary peaks in Figure 2a to 2e vary because of changes in shape and texture.[16d] In Figure 2b, the peak at around 47° shows a shoulder, which is likely a result of some structural distortion. The XRD patterns of nanocrystals synthesized using ODE as a solvent are very similar to those synthesized using OLA (Figure S4). We have determined the *a* and *c* lattice constants as a function of Ga concentration. As expected, both of these values decrease linearly with increasing Ga concentration (Figure S5). We have further used atomic absorption spectroscopy (AAS) to determine the average composition of the nanocrystals. The concentration of both Cu and Ga are close to the expected ratio over the whole composition range, but the In concentration shows a deficiency, especially for CIS (Table S1). The indium deficiency relative to copper and sulfur may be a result of its slower nucleation and incorporation. We have separately prepared near-stoichiometric CIS nanocrystals using an intentional excess of $In(acac)_3$ for the reaction. Interestingly, the XRD pattern for this sample did not show any change in the peak positions as compared to the one with an In deficiency (Figure S6). A similar observation has been reported by Pan et al.[16a] We have also determined the relative composition of sulfur with respect to the cations using energy dispersive X-ray analysis (EDX), with no significant deviation from stoichiometry being observed.

Figure 3a displays the color change of the nanocrystal suspensions in hexane with increasing Ga content, going from black for $CuInS_2$ to yellow for $CuGaS_2$. We have determined the absorbance onset by plotting $(Ah\nu)^2$ versus $h\nu$ (A = absorbance, h = Planck's constant, and ν = frequency) and extrapolating the slope in the band edge region (Figure S7).[31] A plot of the determined band gap versus Ga/(In+Ga) concentration for the nanocrystals synthesized in OLA is shown in Figure 3b. With increasing concentration of Ga, the band gap of the $CuIn_xGa_{1-x}S_2$ nanocrystals increases from 1.53 eV for CIS to 2.48 eV for CGS.

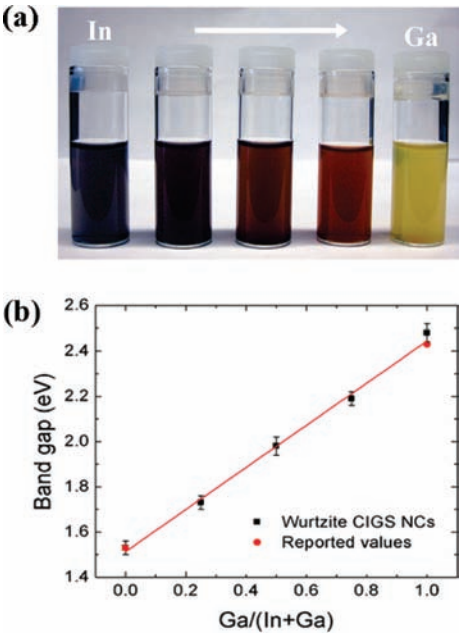

Figure 3. (a) Photographs showing the color evolution of nanocrystal suspensions going from $CuInS_2$ (left) to $CuGaS_2$ (right); (b) plot of band gap of the nanocrystals as a function of Ga/(In+Ga) ratio.

These values are close to the reported values of 1.53 and 2.43 eV[7a] for bulk chalcopyrite $CuInS_2$ and $CuGaS_2$, respectively, with no size confinement effect being observed because of the relatively large size of the nanocrystals. The products synthesized in both OLA and ODE exhibit very similar band gaps (see Table S1).

In conclusion, we have synthesized monodisperse wurtzite-structured $CuIn_xGa_{1-x}S_2$ semiconductor nanocrystals over the entire composition range via a simple solution-based route involving the thermal decomposition of metal-acetylacetonate precursors and their reaction with a mixture of sulfur sources, 1-dodecanethiol and *tert*-dodecanethiol. The morphology of the nanocrystals can be controlled in the form of bullet-like, rod-like, and tadpole-like shapes. As expected, the band gap of the nanocrystals increases linearly with increasing Ga concentration, with the band gap of the end members being close to those in the bulk.[7a] The CIGS nanocrystals readily form colloidal suspensions that can be used as inks for low-cost fabrication of thin-film solar cells.

■ ASSOCIATED CONTENT

Ⓢ Supporting Information. The Table of composition, band gap and lattice constants, TEM images over the entire composition range using OLA and ODE as solvents, XRD pattern of nanocrystals using ODE as solvent, absorption spectra for different compositions. This material is available free of charge via the Internet at http://pubs.acs.org.

■ AUTHOR INFORMATION

Corresponding Author
awang@mint.ua.edu; nzhbao@njut.edu.cn; agupta@mint.ua.edu

■ ACKNOWLEDGMENT

This work was supported by the U.S. Department of Energy, Office of Basic Energy Sciences, Division of Materials Sciences

and Engineering under Award No. DE-FG02-08ER46537, the National Science Foundation under Grant No. CHE-1012850, the Natural Science Foundation of China under Award No. 21006044, and the Key Laboratory of Material-Oriented Chemical Engineering of China under Grant No. KL10-02. As a visiting graduate student from Southeast University, X.Z. was also partially supported by the China Scholarship Council.

REFERENCES

(1) (a) Huynh, W. U.; Dittmer, J. J.; Alivisatos, A. P. *Science* **2002**, *295*, 2425. (b) Gur., I.; Fromer, N. A.; Geier, M. L.; Alivisatos, A. P. *Science* **2005**, *310*, 462.

(2) Kay, A.; Gratzel, M. *Sol. Energy Mater. Sol. Cells* **1996**, *44*, 99.

(3) Guo, Q.; Ford, G. M.; Yang, W.-C.; Walker, B. C.; Stach, E. A.; Hillhouse, H. W.; Agrawal, R. *J. Am. Chem. Soc.* **2010**, *132*, 17384.

(4) Murray, C. B.; Norris, D. J.; Bawendi, M. G. *J. Am. Chem. Soc.* **1993**, *115*, 8706.

(5) (a) Peng, X. G.; Manna, L.; Yang, W. D.; Wickham, J.; Scher, E.; Kadavanich, A.; Alivisatos, A. P. *Nature* **2000**, *404*, 59. (b) Wang, J.; Gudiksen, M. S.; Duan, X.; Cui, Y.; Lieber, C. M. *Science* **2001**, *293*, 1455. (c) Hu, J.; Li, L.-S.; Yang, W.; Manna, L.; Wang, L.-W.; Alivisatos, A. P. *Science* **2001**, *292*, 2060.

(6) (a) Loferski, J. J. *J. Appl. Phys.* **1956**, *27*, 777. (b) Roth, R. S.; Parker, H. S.; Brower, W. S. *Mater. Res. Bull.* **1973**, *8*, 333. (c) Kazmerski, L. L. *Inst. Phys. Conf. Ser.* **1977**, *35*, 217. (d) Wagner, S.; Bridenbaugh, P. M. *J. Cryst. Growth* **1977**, *39*, 151. (e) Romeo, N. *Jpn. J. Appl. Phys.* **1980**, *19*, 5. (f) Cattarin, S.; Pagura, C.; Armelao, L.; Bertoncello, R.; Dietz, N. *J. Electrochem. Soc.* **1995**, *142*, 2818.

(7) (a) Shay, J. L.; Wernick, J. H. *Ternary Chalcopyrite Semiconductors*; Pergamon: Oxford, 1975. (b) Binsma, J. J. M.; Giling, L. J.; Bloem, J. *J. Cryst. Growth* **1980**, *50*, 429. (c) Binsma, J. J. M.; Giling, L. J.; Bloem, J. *Phys. Status Solidi A* **1981**, *63*, 595.

(8) (a) Bodnar, I. V.; Korzun, B. V.; Yasyukevich, L. V. *Russ. J. Inorg. Chem.* **1998**, *43*, 771. (b) Bodnar, I. V.; Yasyukevich, L. V.; Korzoun, B. V.; Karoza, A. G. *J. Mater. Sci.* **1998**, *33*, 183. (c) Ng, M. T.; Boothroyd, C. B.; Vittal, J. J. *J. Am. Chem. Soc.* **2006**, *128*, 7118.

(9) (a) Qi, Y.; Liu, Q.; Tang, K.; Liang, Z.; Ren, Z.; Liu, X. *J. Phys. Chem. C* **2009**, *113*, 3939. (b) Connor, S. T.; Hsu, C.-M.; Weil, B. D.; Aloni, S.; Cui, Y. *J. Am. Chem. Soc.* **2009**, *131*, 4962. (c) Koo, B.; Patel, R. N.; Korgel, B. A. *Chem. Mater.* **2009**, *21*, 1962.

(10) Alonso, M. I.; Wakita, K.; Pascual, J.; Garriga, M.; Yamamoto, N. *Phys. Rev. B* **2001**, *63*, 75203.

(11) Klenk, R.; Klaer, J.; Scheer, R.; Lux-Steiner, M. C.; Luck, I.; Meyer, N.; Ruhle, U. *Thin Solid Films* **2005**, *480*, 509.

(12) Look, D. C.; Manthuruthil, J. C. *J. Phys. Chem. Solids* **1976**, *37*, 173.

(13) (a) Murray, C. B.; Norris, D. J.; Bawendi, M. G. *J. Am. Chem. Soc.* **1993**, *115*, 8706. (b) Heyon, T. *Chem. Commun.* **2003**, *8*, 927. (c) Joo, J.; Na, H. B.; Yu, T.; Yu, J. H.; Kim, Y. W.; Wu, F.; Zhang, J. Z.; Hyeon, T. *J. Am. Chem. Soc.* **2003**, *125*, 11100. (d) Gautam, U. K.; Seshadri, R. *Mater. Res. Bull.* **2004**, *39*, 669.

(14) (a) Zhong, H.; Zhou, Y.; Ye, M.; He, Y.; Ye, J.; He, C.; Yang, C.; Li, Y. *Chem. Mater.* **2008**, *20*, 6434. (b) Zheng, L.; Xu, Y.; Song, Y.; Wu, C. Z.; Zhang, M.; Xle, Y. *Inorg. Chem.* **2009**, *48*, 4003. (c) Courtel, F. M.; Paynter, R. W.; Marsan, B.; Morin, M. *Chem. Mater.* **2009**, *21*, 3752. (d) Long, F.; Wang, W.-M.; Tao, H.-C.; Jia, T.-K.; Li, X.-M.; Zou, Z.-G.; Fu, Z.-Y. *Mater. Lett.* **2010**, *64*, 195.

(15) Xie, R.; Rutherford, M.; Peng, X. *J. Am. Chem. Soc.* **2009**, *131*, 5691.

(16) (a) Pan, D.; An, L.; Sun, Z.; Hou, W.; Yang, Y.; Yang, Z.; Lu, Y. *J. Am. Chem. Soc.* **2008**, *130*, 5620. (b) Norako, M. E.; Franzman, M. A.; Brutchey, R. L. *Chem. Mater.* **2009**, *21*, 4299. (c) Wang, J.-J.; Wang, Y.-Q.; Cao, F.-F.; Guo, Y.-G.; Wan, L.-J. *J. Am. Chem. Soc.* **2010**, *132*, 12218. (d) Kruszynska, M.; Borchert, H.; Parisi, J.; Kolny-Olesiak, J. *J. Am. Chem. Soc.* **2010**, *132*, 15976.

(17) (a) Lu, Q.; Hu, J.; Tang, K.; Qian, Y.; Zhou, G.; Liu, X. *Inorg. Chem.* **2000**, *39*, 1606. (b) Hu, J. Q.; Deng, B.; Wang, C. R.; Tang, K. B.; Qian, Y. T. *Solid State Commun.* **2002**, *121*, 493.

(18) (a) Guo, Q.; Ford, G. M.; Hillhouse, H. W.; Agrawal, R. *Nano Lett.* **2009**, *9*, 3060. (b) Sun, C.; Gardner, J. S.; Long, G.; Bajracharya, C.; Thurber, A.; Punnoose, A.; Rodriguez, R. G.; Pak, J. J. *Chem. Mater.* **2010**, *22*, 2699.

(19) Han, W.; Yi, L.; Zhao, N.; Tang, A.; Gao, M.; Tang, Z. *J. Am. Chem. Soc.* **2008**, *130*, 13152.

(20) (a) Tjong, S. C. Nanocrystalline Materials: Their Synthesis-Structure-Property Relationships and Applications; Elsevier Ltd., 2006. (b) Franzman, M. A.; Perez, V.; Brutchey, R. L. *J. Phys. Chem. C* **2009**, *113*, 630.

(21) Tian, L.; Elim, H. I.; Ji, W.; Vittal, J. J. *Chem. Commun.* **2006**, 4276.

(22) Saatchi, K.; Patrick, B. O.; Orvig, C. *Dalton Trans.* **2005**, 2268.

(23) (a) Wang, Y.-H. A.; Bao, N.; Shen, L.; Padhan, P.; Gupta, A. *J. Am. Chem. Soc.* **2007**, *129*, 12408. (b) Wang, C.; Hou, Y.; Kim, J.; Sun, S. *Angew. Chem., Int. Ed.* **2007**, *46*, 6333.

(24) (a) Vayssieres, L.; Keis, K.; Hagfeldt, A.; Lindquist, S. *Chem. Mater.* **2001**, *13*, 4395. (b) Shen, L.; Bao, N.; Yanagisawa, K.; Zheng, Y.; Domen, K.; Gupta, A.; Grimes, C. A. *J. Solid State Chem.* **2007**, *180*, 213. (c) Shen, L.; Bao, N.; Yanagisawa, K.; Domen, K.; Grimes, C. A.; Gupta, A *J. Phys. Chem. C* **2007**, *111*, 7280.

(25) (a) Manna, L.; Scher, E. C.; Alivisatos, A. P. *J. Am. Chem. Soc.* **2000**, *122*, 12700. (b) Peng, Z. A.; Peng, X. *J. Am. Chem. Soc.* **2002**, *124*, 3343.

(26) (a) Li, X.; Niu, J. Z.; Shen, H.; Xu, W.; Wang, H.; Li, L. S. *Cryst. Eng. Comm.* **2010**, *12*, 4410. (b) Tian, L.; Ng, M. T.; Venkatram, N; Ji, W.; Vittal, J. J. *Cryst. Growth Des.* **2010**, *10*, 1237.

(27) Hu, J.; Zhang, Y.; Liu, B.; Liu, J.; Zhou, H.; Xu, Y.; Jiang, Y.; Yang, Z.; Tian, Z.-Q. *J. Am. Chem. Soc.* **2004**, *126*, 9470.

(28) Binsma, J. J. M.; Giling, L. J.; Bloem, J. *J. Cryst. Growth* **1980**, *50*, 429.

(29) Thangavel, R.; Rajagopalan, M.; Kumar, J. *Phys. Stat. Sol. (B)* **2007**, *244*, 3183.

(30) Lu, X.; Zhuang, Z.; Peng, Q.; Li, Y. *Chem. Commun.* **2011**, *47*, 3141.

(31) (a) Rajaram, P.; Thanagaraj, R.; Sharma, A. K.; Raza, A.; Agnihotri, O. P. *Thin Solid Films* **1983**, *100*, 111. (b) Onnagawa, H.; Miyashita, K. *Jpn. J. Appl. Phys.* **1984**, *23*, 965. (c) Panthani, M. G.; Akhavan, V.; Goodfellow, B.; Dunn, L.; Dodabalapur, A.; Barbara, P. F.; Korgel, B. A. *J. Am. Chem. Soc.* **2008**, *130*, 16770.